CHIN. PHYS. LETT. Vol. 30, No. 11 (2013) 110303

Radio-Frequency Spectra of Ultracold Fermi Gases Including a Generalized GMB Approximation at Unitarity *

RUAN Xiao-Xia(阮小霞)[1,2], GONG Hao(宫昊)[1,3], DU Long(杜龙)[1], JIANG Yu(蒋宇)[4,5], SUN Wei-Min(孙为民)[1,5,6], ZONG Hong-Shi(宗红石)[1,5,6]

[1]*Department of Physics, Nanjing University, Nanjing 210093*
[2]*Faculty of Science, Jiangsu University, Zhenjiang 212013*
[3]*Department of Mathematics and Physics, Bengbu College, Bengbu 233030*
[4]*Center for Statistical and Theoretical Condensed Matter Physics, Zhejiang Normal University, Jinhua 321004*
[5]*State Key Laboratory of Theoretical Physics, Institute of Theoretical Physics, Chinese Academy of Sciences, Beijing 100190*
[6]*Joint Center for Particle, Nuclear Physics and Cosmology, Nanjing 210093*

(Received 27 August 2013)

Taking into account the effect of the generalized Gor'kov and Melik–Barkhudarov (GMB) approximation, we calculate the radio-frequency spectra of balanced and homogeneous ultracold Fermi gases within the framework of the non-self-consistent T-matrix approximation at unitarity in the normal phase. The corresponding equations are numerically calculated on the real frequency axis directly. It is found that our results agree well with the experimental result of the radio-frequency spectroscopy [Phys. Rev. Lett. 101 (2008) 140403].

PACS: 03.75.Ss, 05.30.Fk, 03.75.Hh DOI: 10.1088/0256-307X/30/11/110303

Ultracold Fermi gases provide model systems to study many-body physics owing to their easy tunabilities. This field has been extensively studied theoretically and experimentally.[1–8] Controlling the pairing interaction via Feshbach resonance allows the study of the crossover from Bardeen–Cooper–Schrieffer (BCS) superfluidity to Bose–Einstein condensate (BEC). The interaction strength between atoms can be described by the parameter $(k_{\rm F}a_{\rm s})^{-1}$, where $k_{\rm F}$ is the Fermi wave vector and $a_{\rm s}$ is the s-wave scattering length. In the weak-coupling BCS limit, $(k_{\rm F}a_{\rm s})^{-1} \ll -1$, whereas in the strong-coupling BEC limit, $(k_{\rm F}a_{\rm s})^{-1} \gg +1$. The region $-1 \lesssim (k_{\rm F}a_{\rm s})^{-1} \lesssim +1$ is the crossover region and $(k_{\rm F}a_{\rm s})^{-1} = 0$ is the unitarity limit which is of special importance to understanding the crossover physics.

A fundamental question of ultracold Fermi gases is how to understand the pairing mechanism. In weak coupling BCS limit, pairing and superfluidity emerge simultaneously, whereas in the center of BCS-BEC crossover it is predicted that pairs appear at temperatures T^* higher than the critical temperature for superfluidity and the preformed pairs are usually regarded as the origin of pseudogaps. The study of the pseudogap phenomenon is expected to be helpful for further understanding high-temperature superconductivity. The recent radio-frequency (rf) spectroscopy experiments[9–14] on ultracold Fermi gases provide valuable information on the nature of pairing. In these experiments, a radio-frequency pulse drives atoms from one of two paired spin states into an unoccupied spin state, where they are counted to yield a spectrum of counts versus frequency.[13] The rf spectra are associated with the spectral function of ultracold Fermi gases. The theoretical studies of rf spectra have been performed by many authors.[15–23] However, the effect of the induced interaction, also called the GMB approximation, which was first considered by Gor'kov and Melik-Barkhudarov (GMB),[24] has not been taken into account in their studies of the spectral function through which we can calculate rf spectra.

Yu and coworkers[25] considered the generalized GMB approximation in the Nozières and Schmitt-Rink (NSR)[26] framework to study ultracold Fermi gases. The NSR approach is equivalent to expanding the fermion propagator to the lowest order in the self-energy when one calculates the number equation via the fermion propagator. If the fluctuation corrections are important as in the BCS-BEC crossover, a better treatment might be to include the self-energy to all orders. This is exactly the non-self-consistent T-matrix approximation (nTMA) framework as adopted in Ref. [27]. In this Letter, taking into account the generalized GMB approximation in the nTMA framework, we calculate the rf spectra of balanced and homogeneous ultracold Fermi gases in the normal phase at unitarity. We compare our results with the experimental results of rf spectra in Ref. [14] and the results from the NSR theory and the extended BCS-Leggett theory obtained by Chien and coworkers in Ref. [28]. It is found that our results agree well with the experimental result after taking into account induced interaction. Throughout this study, we take $\hbar = k_{\rm B} = 1$.

We consider three-dimensional uniform Fermi gases with an equal number of particles in the two different hyperfine states described by pseudospins $\sigma =\uparrow$

*Supported in part by the National Natural Science Foundation of China under Grants Nos 11275097, 10935001 and 11075075, and the Research Fund for the Doctoral Program of Higher Education under Grant No 2012009111002.
**Corresponding author. Email: zonghs@chenwang.nju.edu.cn
© 2013 Chinese Physical Society and IOP Publishing Ltd

and $\downarrow$. The system with a broad Feshbach resonance can be modeled by the Hamiltonian

$$H-\mu N=\sum_{\boldsymbol{k},\sigma}\xi_{\boldsymbol{k}}c^{\dagger}_{\boldsymbol{k}\sigma}c_{\boldsymbol{k}\sigma} - U\sum_{\boldsymbol{q}\boldsymbol{k}\boldsymbol{k}'}c^{\dagger}_{\boldsymbol{k}+\boldsymbol{q}/2\uparrow}c^{\dagger}_{\boldsymbol{k}+\boldsymbol{q}/2\downarrow}c_{-\boldsymbol{k}'+\boldsymbol{q}/2\downarrow}c_{\boldsymbol{k}'+\boldsymbol{q}/2\uparrow}, \tag{1}$$

where $c_{\boldsymbol{k}\sigma}$ represents the annihilation operator for a Fermi atom with pseudospin σ and kinetic energy $\xi_{\boldsymbol{k}}=\varepsilon_{\boldsymbol{k}}-\mu$ with μ being the chemical potential. The pairing interaction $-U$ (which is negative) is tunable. When we calculate some physical quantity, we will relate $-U$ to the observable quantity, i.e., the s-wave scattering length $a_{\rm s}$ via

$$\frac{1}{-U}=\frac{m}{4\pi a_{\rm s}}-\sum_{\boldsymbol{k}}\frac{1}{2\varepsilon_{\boldsymbol{k}}}. \tag{2}$$

The induced interaction was considered originally by GMB[24] in the BCS limit. Yu and coworkers[25] used the generalized GMB approximation in the BCS-BEC crossover. For a scattering process $p_1+p_2\to p_3+p_4$, the induced interaction considered by Yu and coworkers is

$$U_{\rm ind}(p_1,p_2;p_3,p_4)=-\frac{U^2\chi(p_1-p_4)}{1-U\chi(p_1-p_4)} =-\frac{U^2\chi(q)}{1-U\chi(q)}=U_{\rm ind}(q), \tag{3}$$

where $p_i=(\boldsymbol{k}_i,i\omega_{n_i})$ with $\boldsymbol{k}$ being the wave vector and $\omega_n=(2n+1)\pi/\beta=(2n+1)\pi T$ being the fermion Matsubara frequency, and $q=(\boldsymbol{q},i\nu_n)$ with ν_n being the boson Matsubara frequency. The polarization function χ is

$$\chi(q)=T\sum_{\boldsymbol{k},i\omega_n}\mathcal{G}_0(p)\mathcal{G}_0(p+q)=\sum_{\boldsymbol{k}}\frac{f(\xi_{\boldsymbol{k}})-f(\xi_{\boldsymbol{k}+\boldsymbol{q}})}{i\nu_n+\xi_{\boldsymbol{k}}-\xi_{\boldsymbol{k}+\boldsymbol{q}}}, \tag{4}$$

where $\mathcal{G}_0(p)=\mathcal{G}_0(\boldsymbol{k},i\omega_n)=1/(i\omega_n-\xi_{\boldsymbol{k}})$ is the Matsubara function of a noninteracting fermion, and $f(\xi_{\boldsymbol{k}})=1/[\exp(\beta\xi_{\rm k})+1]$ is the Fermi distribution function.

The effective interaction is the sum of the bare interaction and the induced interaction. It is given by

$$-U_{\rm eff}(q)=\frac{-U}{1-U\chi(q)}. \tag{5}$$

Here χ (and hence $-U_{\rm eff}$) is a function of the momentum and the frequency.

Following the approach used in Ref. [25], we replace $\chi(q)$ in Eq. (5) by its average $\langle\chi\rangle$. This leads to

$$-U_{\rm eff}=\frac{-U}{1-U\langle\chi\rangle}. \tag{6}$$

We borrow the result of the average of χ from Ref. [25]. When $\mu>0$, the average of χ is

$$\langle\chi\rangle=\frac{m}{4\pi^2}\int_{-1}^{1}d\cos\theta\int_0^{\infty}dk\frac{k}{k'}f_k\ln\left|\frac{k'-2k}{k'+2k}\right|, \tag{7}$$

where $k'=k_{\rm F}\sqrt{2(1+\cos\theta)}$, and $f_k=f(\xi_{\boldsymbol{k}})$ is the Fermi distribution function. When μ becomes negative on the BEC side, the Fermi surface disappears, and the average of χ is

$$\langle\chi\rangle=-\frac{m}{2\pi^2}\int_0^{\infty}dkf_k. \tag{8}$$

The single-particle thermal Green's function is

$$\mathcal{G}_{\boldsymbol{k}}(i\omega_n)=\frac{1}{i\omega_n-\xi_{\boldsymbol{k}}-\Sigma(\boldsymbol{k},i\omega_n)}. \tag{9}$$

Different approximation schemes lead to different self-energy correction $\Sigma(\boldsymbol{k},i\omega_n)$. In this study we adopt nTMA as in Ref. [27]. In the nTMA, the self-energy function $\Sigma(\boldsymbol{k},i\omega_n)$ which describes pairing fluctuations represented by Fig. 1 is

$$\Sigma(\boldsymbol{k},i\omega_n)=T\sum_{\boldsymbol{q},i\nu_n}\Gamma(\boldsymbol{q},i\nu_n)\mathcal{G}^0_{\boldsymbol{q}-\boldsymbol{k}}(i\nu_n-i\omega_n)e^{i(\nu_n-\omega_n)\delta}, \tag{10}$$

where ν_n is the boson Matsubara frequency and $\Gamma(\boldsymbol{q},i\nu_n)$ is the particle-particle scattering matrix, which is depicted in Fig. 2.

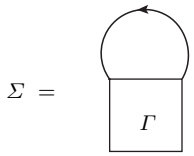


Fig. 1. Self-energy function $\Sigma(\boldsymbol{k},i\omega_n)$ in the nTMA. The solid line represents the free fermion propagator.

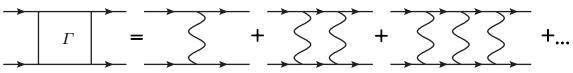


Fig. 2. Particle-particle scattering matrix $\Gamma(\boldsymbol{q},i\nu_n)$ in the nTMA. The straight and wavy lines represent the free fermion propagator and the effective interaction in Eq. (6), respectively.

The self-energy is formulated for Matsubara frequencies on the imaginary axis. One can use the Padé approximation to continue the self-energy to a real frequency axis. In this study, we adopt another method. We calculate the imaginary part of the retarded self-energy $\mathrm{Im}\Sigma^R(\boldsymbol{k},\omega)$ via the real frequency formalism

$$\mathrm{Im}\Sigma^R(\boldsymbol{k},\omega)=\sum_{\boldsymbol{q}}[b(\omega+\xi_{\boldsymbol{q}-\boldsymbol{k}})+f(\xi_{\boldsymbol{q}-\boldsymbol{k}})] \times\mathrm{Im}[\Gamma^R(\boldsymbol{q},\omega+\xi_{\boldsymbol{q}-\boldsymbol{k}})], \tag{11}$$

where $f(x)=1/(e^{\beta x}+1)$ is the Fermi distribution function and $b(x)=1/(e^{\beta x}-1)$ is the Bose distribution function. The real part of the retarded self-energy $\mathrm{Re}\Sigma^R(\boldsymbol{k},\omega)$ can be obtained via the Kramers–Kronig relation. This approach can avoid the difficulty of analytical continuation of the numerical results from imaginary frequency to real frequency.

The single-particle spectral function which is of great importance to calculating the rf spectra is determined by the imaginary part of the retarded Green's function via

$$A(\boldsymbol{k},\omega) = -\frac{1}{\pi}\mathrm{Im}[\mathcal{G}(\boldsymbol{k}, i\omega_n \to \omega + i\delta)]. \tag{12}$$

In terms of the real part and the imaginary part of the retarded self-energy, $A(\boldsymbol{k},\omega)$ can be expressed as

$$A(\boldsymbol{k},\omega) = -\frac{1}{\pi}\frac{\mathrm{Im}\Sigma^R(\boldsymbol{k},\omega)}{[\omega - \xi_{\boldsymbol{k}} - \mathrm{Re}\Sigma^R(\boldsymbol{k},\omega)]^2 + [\mathrm{Im}\Sigma^R(\boldsymbol{k},\omega)]^2}. \tag{13}$$

The imaginary part of the retarded self-energy is crucial to the calculation of spectral function. In order to obtain $\mathrm{Im}\Sigma^R(\boldsymbol{k},\omega)$ via Eq. (11), now we focus on the particle-particle scattering matrix $\Gamma(\boldsymbol{q}, i\nu_n)$. The expression is

$$\begin{aligned}\Gamma(\boldsymbol{q}, i\nu_n) &= \frac{-U_{\mathrm{eff}}}{1 - U_{\mathrm{eff}}\Pi(\boldsymbol{q}, i\nu_n)} \\ &= \left\{\frac{m}{4\pi a_{\mathrm{s}}} - \sum_{\boldsymbol{k}}\frac{1}{2\varepsilon_{\boldsymbol{k}}} + \langle\chi\rangle + \Pi(\boldsymbol{q}, i\nu_n)\right\}^{-1},\end{aligned} \tag{14}$$

where the pair propagator $\Pi(\boldsymbol{q}, i\nu_n)$ is given by

$$\begin{aligned}\Pi(\boldsymbol{q}, i\nu_n) &= T\sum_{\boldsymbol{k}, i\omega_n}\mathcal{G}^0_{\boldsymbol{k}+\boldsymbol{q}/2}(i\nu_n + i\omega_n)\mathcal{G}^0_{-\boldsymbol{k}+\boldsymbol{q}/2}(-i\omega_n) \\ &= \sum_{\boldsymbol{k}}\frac{1 - f(\xi_{\boldsymbol{k}+\boldsymbol{q}/2}) - f(\xi_{\boldsymbol{k}-\boldsymbol{q}/2})}{\xi_{\boldsymbol{k}+\boldsymbol{q}/2} + \xi_{\boldsymbol{k}-\boldsymbol{q}/2} - i\nu_n}.\end{aligned} \tag{15}$$

Performing the analytical continuation $i\nu_n \to z + i\delta$, we arrive at

$$\Pi(\boldsymbol{q}, z + i\delta) = \sum_{\boldsymbol{k}}\frac{1 - f(\xi_{\boldsymbol{k}+\boldsymbol{q}/2}) - f(\xi_{\boldsymbol{k}-\boldsymbol{q}/2})}{\xi_{\boldsymbol{k}+\boldsymbol{q}/2} + \xi_{\boldsymbol{k}-\boldsymbol{q}/2} - z - i\delta}. \tag{16}$$

The imaginary part of $\Pi(\boldsymbol{q}, z + i\delta)$ is

$$\begin{aligned}\mathrm{Im}\Pi(\boldsymbol{q}, z + i\delta) &= \frac{m\sqrt{m}}{4\pi\beta\sqrt{E^0_q}}\theta(z + 2\mu - E^0_q) \\ &\times \ln\frac{\cosh\dfrac{\beta}{2}\left[\dfrac{z}{2} + \sqrt{(z + 2\mu - E^0_q)E^0_q}\right]}{\cosh\dfrac{\beta}{2}\left[\dfrac{z}{2} - \sqrt{(z + 2\mu - E^0_q)E^0_q}\right]},\end{aligned} \tag{17}$$

where $E^0_q = q^2/4m$, and $\theta(x)$ is the step function. Then, we can obtain the imaginary part of $\Gamma(\boldsymbol{q}, z + i\delta)$ via Eq. (14).

In this study, we focus on the normal state of ultracold Fermi gases. Knowledge of T_c is required. The critical temperature T_c can be obtained from the Thouless criterion $\Gamma(\boldsymbol{q} = 0, i\nu_n = 0, T = T_c)^{-1} = 0$, which gives

$$\frac{m}{4\pi a_{\mathrm{s}}} + \langle\chi\rangle = \sum_{\boldsymbol{k}}\left[\frac{1}{2\varepsilon_{\boldsymbol{k}}} - \frac{1}{2(\varepsilon_{\boldsymbol{k}} - \mu)}\tanh\frac{\xi_{\boldsymbol{k}}}{2T}\right]. \tag{18}$$

There are two important differences between the usual BCS calculation and the BCS-BEC crossover. First, in the BCS-BEC crossover there is no explicit cutoff as in the BCS theory, and we have to regularize the ultraviolet divergence via Eq. (2). Second, the chemical potential μ deviates from the Fermi energy ε_{F} and it is determined via the number of Fermi atoms,

$$N = 2T\sum_{\boldsymbol{k}, i\omega_n} e^{i\omega_n\delta}\mathcal{G}_{\boldsymbol{k}}(i\omega_n). \tag{19}$$

By solving the coupled equations, Eqs. (18) and (19), we obtain the superfluid transition temperature $T_c = 0.218T_{\mathrm{F}}$ and the chemical potential $\mu(T = T_c)$ is $0.631\varepsilon_{\mathrm{F}}$ at unitarity.[29] The spectral function at the transition temperature can be determined with the obtained T_c and $\mu(T = T_c)$. For $T > T_c$, by solving the number equation [Eq. (19)] only, we can obtain the chemical potential for a certain T. In terms of the given T and the obtained chemical potential, the spectral function can be determined.

In the rf experiments, three different hyperfine states are involved. The two lowest states $|1\rangle$ and $|2\rangle$ participate in the superfluid pairing and the higher state $|3\rangle$ is unoccupied initially. The Hamiltonian for $|3\rangle$ is $H_3 - \mu_3 N_3 = \sum_{\boldsymbol{p}}(\varepsilon_{\boldsymbol{p}} + \omega_3 - \mu_3)b^\dagger_{\boldsymbol{p}}b_{\boldsymbol{p}}$. Here, $\varepsilon_{\boldsymbol{p}}$ is the atomic kinetic energy, ω_3 is the energy splitting between $|3\rangle$ and $|2\rangle$, μ_3 is the chemical potential of $|3\rangle$, and $b_{\boldsymbol{p}}$ is the annihilation operator for a Fermi atom in $|3\rangle$.

An rf pulse excites atoms from the state $|2\rangle(\equiv|\uparrow\rangle)$ to another unoccupied state $|3\rangle$. The transition from $|2\rangle$ to $|3\rangle$ is described by the Hamiltonian[30] $H_T = t_{\mathrm{F}}\sum_{\boldsymbol{k}}(e^{-i\omega_{\mathrm{L}}t}b^\dagger_{\boldsymbol{k}+\boldsymbol{q}_{\mathrm{L}}}c_{\boldsymbol{k}\uparrow} + \mathrm{H.c.})$, where t_{F} is a transfer matrix element between $|2\rangle$ and $|3\rangle$, which is taken to be a constant, and $\boldsymbol{q}_{\mathrm{L}}$ and ω_{L} are the momentum and energy of the rf pulse. The momentum of the radio frequency photon $\boldsymbol{q}_{\mathrm{L}}$ is negligible compared with the typical momenta of the atoms, and the momenta of the outcoupled atoms are equal to that of the original atom states.[13] For simplicity, we ignore the final-state effects as in Ref. [28]. The rf current defined as $I = \langle\dot{N}_3\rangle$ can be obtained from the linear response theory and it is given by Refs. [28,30]

$$I(\nu) = 2\pi t^2_{\mathrm{F}}\sum_{\boldsymbol{k}} A(\boldsymbol{k},\omega)f(\omega)|_{\omega=\xi_k-\nu}, \tag{20}$$

where $\nu = \omega_{\mathrm{L}} - \omega_3$ is the rf detuning, $f(\omega)$ is the Fermi distribution function, and $A(\boldsymbol{k},\omega)$ is the spectral function including the generalized GMB approximation.

In order to compare our results with those in Ref. [28] and the corresponding experimental result in Ref. [14] (see the supplemental materials), we normalize each curve by its maximum and align the maximum on the horizontal axis as performed by Chien and coworkers.[28] In the present work we aim at comparing rf spectroscopies in the normal phase and in the unitarity limit.

In Fig. 3 we show the calculated rf spectra in the present work, the experimental data of Schirotzek *et al.* (supplemental materials in Ref. [14]), the results obtained from the NSR theory and the extended BCS-Leggett theory (GG_0) by Chien and coworkers in Ref. [28]. We take the experimental data at $T = 0.22T_{\rm F}, 0.34T_{\rm F}, 0.55T_{\rm F}$. In order to compare the results conveniently, the rf spectra obtained by us are also calculated at the same set of temperatures. The calculated rf spectra for a homogeneous and balanced system at unitarity show a single peak, which is different from the result of the extended BCS-Leggett calculation. The single peak is consistent with the experimental result and the result of NSR theory. However, the rf spectra obtained from NSR theory in Ref. [28] show a broader peak as compared to experiments. The same phenomenon also exists in the GG t-matrix calculation.[31] From Fig. 3, we see that compared to experiments, after taking into account the generalized GMB approximation, a more satisfactory result can be obtained without slightly overestimating the width of the peak.

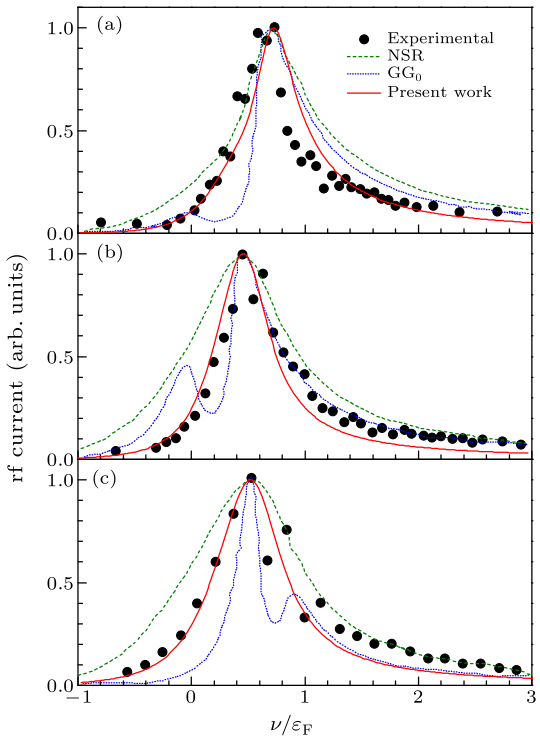


Fig. 3. Radio-frequency spectra at unitarity for different temperatures in the normal phase. The (red) solid lines are our results of rf spectra obtained after taking into account the generalized GMB approximation in the nTMA framework, the (black) solid dots are the experimental data of Schirotzek *et al.* (supplemental materials of Ref. [14]), the (green) dashed lines are the NSR results from Ref. [28], and the (blue) dotted lines are the results obtained from the extended BCS-Leggett (GG_0) theory by Chien and coworkers in Ref. [28]. The values of $T/T_{\rm F}$ are (a) 0.22 (0.24 for the curve from NSR theory), (b) 0.34, and (c) 0.55.

In summary, we have studied the rf spectra of ultracold Fermi gases at unitarity in the normal phase including the generalized GMB approximation in the nTMA framework, which combines a generalized version of the usual GMB correction with a theoretical framework for pairing and superfluidity, which incorporates pairing fluctuations. The obtained rf spectra for a homogeneous and balanced system show a single peak, which is consistent with experiments. A more satisfactory result is obtained without slightly overestimating the width of the peak that emerges in the extended BCS-Leggett calculation and GG t-matrix theory.

References

[1] Bloch I, Dalibard J and Zwerger W 2008 *Rev. Mod. Phys.* **80** 885
Giorgini S, Pitaevskii L P and Stringari S 2008 *Rev. Mod. Phys.* **80** 1215
[2] Greiner M, Regal C A and Jin D S 2003 *Nature* **426** 537
[3] Regal C A, Greiner M and Jin D S 2004 *Phys. Rev. Lett.* **92** 040403
[4] Jochim S et al 2003 *Science* **302** 2101
[5] Bartenstein M, Altmeyer A, Riedl S, Jochim S, Chin C, Denschlag J H and Grimm R 2004 *Phys. Rev. Lett.* **92** 120401
[6] Bartenstein M, Altmeyer A, Riedl S, Jochim S, Chin C, Denschlag J H and Grimm R 2004 *Phys. Rev. Lett.* **92** 203201
[7] Zwierlein M W, Stan C A, Schunck C H, Raupach S M F, Kerman A J and Ketterle W 2004 *Phys. Rev. Lett.* **92** 120403
[8] Kinast J, Hemmer S L, Gehm M E, Turlapov A and Thomas J E 2004 *Phys. Rev. Lett.* **92** 150402
[9] Chin C, Bartenstein M, Altmeyer A, Riedl S, Jochim S, Denschlag J H and Grimm R 2004 *Science* **305** 1128
[10] Shin Y, Schunck C H, Schirotzek A and Ketterle W 2007 *Phys. Rev. Lett.* **99** 090403
[11] Schunck C H, Shin Y, Schirotzek A, Zwierlein M W and Ketterle W 2007 *Science* **316** 867
[12] Schunck C H, Shin Y I, Schirotzek A and Ketterle W 2008 *Nature* **454** 739
[13] Stewart J T, Gaebler J P and Jin D S 2008 *Nature* **454** 744
[14] Schirotzek A, Shin Y I, Schunck C H and Ketterle W 2008 *Phys. Rev. Lett.* **101** 140403
[15] Kinnunen J, Rodriguez M and Törmä P 2004 *Science* **305** 1131
[16] He Y, Chen Q J and Levin K 2005 *Phys. Rev.* A **72** 011602 (R)
[17] Baym G, Pethick C J, Yu Z and Zwierlein M W 2007 *Phys. Rev. Lett.* **99** 190407
[18] Punk M and Zwerger W 2007 *Phys. Rev. Lett.* **99** 170404
[19] He Y, Chien C C, Chen Q J and Levin K 2008 *Phys. Rev.* A **77** 011602(R)
[20] Perali A, Pieri P and Strinati G C 2008 *Phys. Rev. Lett.* **100** 010402
[21] Basu S and Mueller E J 2008 *Phys. Rev. Lett.* **101** 060405
[22] Massignan P, Bruun G M and Stoof H T C 2008 *Phys. Rev.* A **77** 031601 (R)
[23] Massignan P, Bruun G M and Stoof H T C 2008 *Phys. Rev.* A **78** 031602(R)
[24] Gor'kov L P and Melik-Barkhudarov T K 1961 *Sov. Phys. JETP* **13** 1018
[25] Yu Z Q, Huang K and Yin L 2009 *Phys. Rev.* A **79** 053636
[26] Noziéres P and Schmitt-Rink S 1985 *J. Low Temp. Phys.* **59** 195
[27] Tsuchiya S, Watanabe R and Ohashi Y 2009 *Phys. Rev.* A **80** 033613
[28] Chien C C et al 2010 *Phys. Rev.* A **81** 023622
[29] Ruan X X et al 2013 *Phys. Rev.* A **87** 043608
[30] Tsuchiya S et al 2011 *Phys. Rev.* A **84** 043647
[31] Haussmann R et al 2009 *Phys. Rev.* A **80** 063612